ACCOUNTS
of chemical research

Local Ordering in Lead-Based Relaxor Ferroelectrics

DARREN J. GOOSSENS*
Research School of Chemistry, Australian National University, Canberra 0200, Australia

RECEIVED ON MARCH 13, 2013

CONSPECTUS

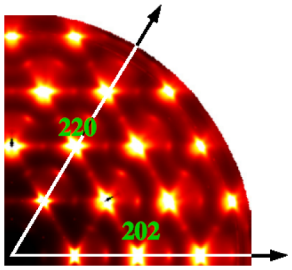

Lead-based ferroelectric materials are both well-studied and widely used and have a wide range of applications from ultrasonics to energy harvesting and beyond. However, the use of Pb-containing materials is environmentally undesirable, due to the toxicity of lead. This is particularly highlighted by the disposal of Pb-based devices when their lifespan is through. Because of this large drawback, chemists have been searching for Pb-free ferroic materials that can replace PZN ($PbZn_{1/3}Nb_{2/3}O_3$), PMN ($PbMg_{1/3}Nb_{2/3}O_3$), PZT ($PbZr_{1-x}Ti_xO_3$), and all their derivatives.

Underlying much of materials chemistry is the idea that function arises from structure, so if we can determine the structure of a material, we can understand how its useful properties arise. This understanding can then lead to the tuning of these properties and the development of new materials. However, the question arises: What is meant by structure? Conventionally, structure is determined by X-ray or neutron diffraction, in which the Bragg peak intensities are measured and a unit cell is determined. In many materials, local ordering, order that persists only for few unit cells or nanometers, is important in determining the physical properties. This is very much the case in the relaxor ferroelectrics, an important class of functional oxides. Indeed, disorder, randomness, and short-range order (SRO) are all invoked to help explain many of the key properties.

The local order in Pb-based ferroelectrics has been extensively studied, with the most definitive probe being single-crystal diffuse scattering. In this Account, I outline the current debate on the nature of the local order and explore how this information can inform the search for lead-free materials. Local order, as distinct from the overall average order revealed by conventional techniques, relates more closely to the crystal chemistry of the individual ions and so appears to give a better insight into how the crystal chemistry leads to the ferroelectric properties.

1. Introduction

The Pb-based ferroelectric materials are a well-studied and widely used class of materials. They find applications in ultrasonics, energy harvesting, accelerometers, and elsewhere,[1−5] where their combination of large polarization, low dielectric loss, and large piezoelectric strain make them key parts of many valuable hi-tech industries. Clearly, however, the use of Pb-containing materials has a number of environmental drawbacks related to the toxicity of lead. This is particularly true in manufacturing the devices and disposing of them when their lifespan is passed. Because piezoelectric materials can be used to "harvest" the energy of waste motion (for example, vibration in a walkway or dance floor[3]) and convert it into electricity, they are potentially very useful in increasing energy efficiency and reducing carbon emissions. However, it is undesirable to incorporate Pb-containing materials into devices and even infrastructure such as buildings and footpaths. Hence the search for Pb-free ferroic materials that can replace PZN ($PbZn_{1/3}Nb_{2/3}O_3$), PMN ($PbMg_{1/3}Nb_{2/3}O_3$), PZT ($PbZr_{1-x}Ti_xO_3$), and all their derivatives and related materials is a major and ongoing effort.

Ferroelectricity in oxides is generally related to displacement of ions such that there is a local separation between the center of the distribution of the positive and negative charge. For example, in perovskite $BaTiO_3$, where Ba is the 12-fold coordinated A-site cation and Ti the 6-fold coordinated B-site cation, the Ti^{4+} ion shows a strong positive charge, so if this ion is displaced in parallel away from the center of its octahedral environment (Figure 1), the crystal obtains a net polarization.

In a relaxor ferroelectric, the ferroelectric phase transition is broad and frequency dependent. This behavior is

Published on the Web 06/04/2013 www.pubs.acs.org/accounts
10.1021/ar400073w

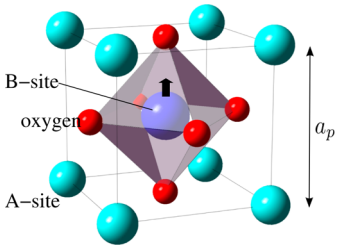

FIGURE 1. A parent perovskite cube, lattice parameter a_p, showing the A-site and B-site cations and oxygen atoms. The thick arrow shows a displacement of the B-site cation (Ti^{4+} in $BaTiO_3$) that would result in a net polarization of the unit cell.

thought to come about through disorder in the crystal structure, the classic examples being PZN and PMN, where chemical disorder on the B-site results in a wide range of environments for the polar A-site atoms, in these cases Pb.

The very existence of ferroelectricity implies that the displacing atoms are interacting in some way. The presence of disorder means that these interactions do not always induce long-range order but can result in local ordering. This also means that the global average ordering as revealed by conventional crystallographic studies is really an average over many local environments and so is not necessarily highly reflective of the local crystal chemistry that is responsible for the interesting and useful physical properties.

Gaining information about local structure is not simple. The tools of conventional crystallography, and the very idea of a single repeating unit cell that defines the structure, are inadequate. Techniques such as X-ray absorption fine structure (XAFS) and X-ray absorption near-edge structure (XANES) can deliver nearest-neighbor coordination information, but for exploring structural correlations that persist for a significant number of unit cells, a length scale of nanometers to tens of nanometers, the analysis of *diffuse scattering* of X-rays, neutrons, and electrons is a technique of great power. Crystallography that goes beyond the average structure is a vibrant growth area in the field.[6−8] Whether making use of single crystal or powder samples, the technique relies on measuring diffracted intensity not just on the Bragg positions but at a wide range of scattering vectors.

Conventional diffraction experiments work primarily by determining the intensities of Bragg reflections. These obey Bragg's law, $n\lambda = 2d \sin\theta$, where θ is half the angle through which the radiation is diffracted, d is the spacing between planes of atoms, n is an integer, and λ is the wavelength.

Bragg reflection will occur when $\mathbf{Q} = \mathbf{G}$, where $\mathbf{G}$ is a vector of the reciprocal lattice and $\mathbf{Q}$ is the scattering vector, $|\mathbf{Q}| = 4\pi \sin\theta/\lambda$. If the desire is to synthesize the crystal structure from Fourier components, this experiment measures intensities associated with a small subset of the possible Fourier components, those that lie on the reciprocal lattice. The reciprocal lattice is calculated from the unit cell of the long-range ordered average structure, so measuring these intensities can tell us only about this average structure, usually described by a conventional unit cell. This average structure is a series of single-body averages. It can tell us that a given site is at a particular point, shows particular atomic displacement parameters (ADPs), and is occupied by certain types of atoms in some ratio. It cannot tell us how a site's behavior or occupancy influences its neighbors.

Diffuse scattering is named so because it is usually broad in reciprocal space, that is, diffuse. It is coherently scattered intensity not restricted to the Bragg peaks. As such, measuring it samples Fourier components that are not solely related to the single-body average structure, so insight can be obtained into two-body correlations in a crystalline material.[9,10] These correlations may exist between atoms, molecules, and, in neutron diffraction, magnetic moments.[11]

Figure 2 shows an example of single-crystal diffuse scattering (SCDS) measured for the layered chalcogenide $NiPS_3$. For this material and related ones, diffuse scattering of X-rays was used to show how the layers in the structure can sheer relative to each other, giving rise to the strong vertical streaks of scattering in Figure 2a, while electron diffuse scattering showed that when Mg is doped into the material, it tends to cluster rather than alternate with the Ni.[12] In the first case, the diffuse scattering is sensitive to how one body moves relative to another, and in the second case, it is sensitive to the occupancy of one site compared with another. These are two-body correlations. The diffuse scattering is sensitive to the "average two-body structure" where conventional diffraction gives the "average single-body structure". Even diffuse scattering is not sensitive to multibody correlations, unless phase can be retrieved.[13]

Conventional structure determination allows great insight into the relationship between structure and the useful properties of the material. However, there are cases where the properties, or even the structure itself, cannot easily be explained in terms of the single-body average. This average may be chemically unlikely; it may be an unphysical average over a multitude of reasonable local configurations. An example in a molecular system is *para*-terphenyl,[14−16] which at room temperature appears to consist of three coplanar phenyl rings, yet in this configuration the H···H bonds within the molecule, illustrated in Figure 3, are prohibitively short. In practice, in every molecule the central ring is rotated relative to the plane of the outer rings, yet when averaged across the crystal the molecules appear flat.

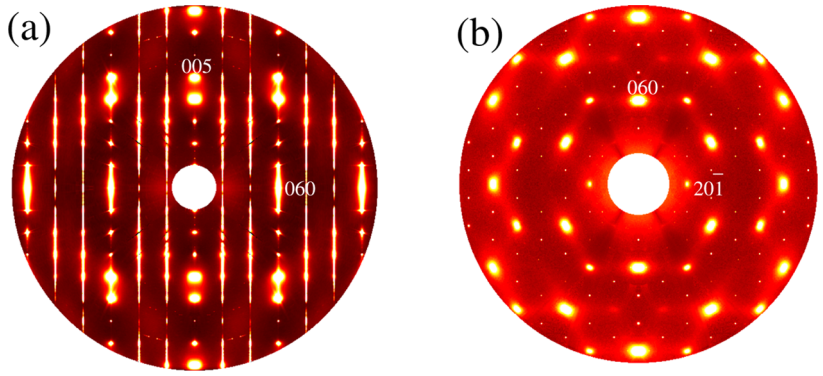

FIGURE 2. Diffuse scattering from $NiPS_3$,[12] showing strong thermal diffuse scattering around Bragg positions plus streaks due to stacking fault-like structures. *hkl*s are given for some peaks to indicate directions and scales in reciprocal space. Images are false-color maps where white is high intensity (including overexposed pixels) and black is low (or pixels absent from data due to experimental coverage or data correction). Panel a shows the 0*kl* cut, while panel b shows a slice in which b^* is vertical and $2a^*-c^*$ is horizontal.

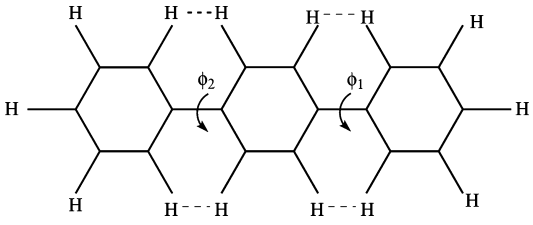

FIGURE 3. A single molecule of *para*-terphenyl, showing the H···H contact vectors that are too short when the phenyl rings are coplanar and that drive the molecule into a twisted conformation even though the average appears flat.

For ferroelectric oxides founded on Pb^{2+}, the polarization mechanism may be based on the Pb environment being too large and the ion being polar, such that it satisfies its bonding requirements by shifting off-center.[17,18] Two possible displacement schemes, shifts along the 12 $\langle 011 \rangle_c$ directions and the 8 $\langle 111 \rangle_c$ directions, are illustrated in Figure 4.

If the ions displace in equal numbers along each of the $\langle 011 \rangle_c$ directions, for example, then the average position is preserved, but the site is now disordered. If these shifts are correlated from site to site, then local ordering exists and diffuse scattering will arise. However, in fitting diffraction data, it may be possible to model the overall average distribution of ions by using a single site at the average position plus anisotropic ADPs. This means that the average single-body structure may not capture important details. The single-body average structure of $PbZr_{1-x}Ti_xO_3$ (PZT) has been heavily studied,[19−23] and at room temperature, powder diffraction data can be extremely well-fitted by a dual-phase model with a rhombohedral *R*3*c* and a monoclinic *Cm* component, with the fraction of *Cm* increasing with Ti concentration.[23] Other results show that on driving the system into the cubic phase at elevated temperatures the Pb atoms show disorder.[24] The presence of structured diffuse scattering at room temperature in electron diffraction[25−28] definitively shows that the correct single-body average model *must* allow for disorder. Therefore, it seems that the powder diffraction is insensitive to the disorder; the dual-phase fits are extremely impressive[23] yet *must* be omitting important structural information.

2. Modeling Diffuse Scattering

When relatively few modulations can describe the diffuse distribution, it is possible to use a modulation wave approach[29] or, in real space, short-range order (SRO) parameters such as Cowley parameters[30] to describe the diffuse scattering and SRO. If the diffuse scattering is the result of some modulation in composition or displacement that can be described analytically, then it may be possible to derive an analytical expression for the locus of diffuse intensity.[31]

Similarly, some insight may be gained by Fourier transforming a representation of a defect or a domain or some other structural motif. For example, a one-dimensional chain of correlated atoms will give rise to sheets of diffuse scattering, while two-dimensional domains will give rise to rods. This is an important tool in qualitatively determining what structural features may be present in the material. However useful, such approaches can be misleading. While it is true that the Fourier transform of a planar domain is indeed a rod of scattering, mathematically that does not necessarily imply that a model containing well-defined static domains is the only one that can produce such features.[32,33] In such cases, it is necessary to bring in additional information beyond that provided by the diffuse scattering.

When one considers large two-dimensional (2D) sections and even large 3D volumes of reciprocal space (which can be collected using modern facilities such as synchrotrons

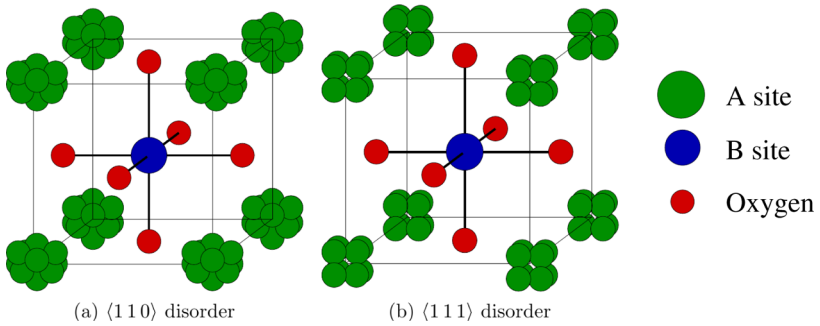

FIGURE 4. Displacement schemes in $PbZr_{1-x}Ti_xO_3$ showing (a) the 12 $\langle 011 \rangle_c$ sites and (b) the 8 $\langle 111 \rangle_c$ sites across which the Pb^{2+} ions are thought to be split, depending on composition, at 850 K (see Figure 6). Subscript *c* indicates indexing based on the parent cubic perovskite cell.

and pulsed neutron sources), the modeling of diffuse scattering is not a routine task. Some toolbox programs are available for modeling diffuse scattering,[34−37] but the wide variety of types of local ordering, from simple chemical substitution to complexities of molecular conformations, militates against the development of an easy-to-use software package that can be rapidly learned by a nonexpert. Such a development is to be desired, and steps continue to be taken in that direction.[34,36,38]

Diffuse scattering can be interpreted in a number of ways. A heuristic approach can often be used by an experienced researcher[39−41] to isolate the key disorder mechanisms, qualitatively at least. This may be buttressed by Monte Carlo (MC) modeling, which is a very flexible numerical modeling approach.[42]

MC modeling in this context comes in two varieties, conventional MC and "reverse MC" (RMC).[43] In both cases, a model crystal many unit cells in size is constructed, usually based on a known average structure, and atoms or molecules are shifted or swapped.

In MC, a system energy is defined in terms of the atomic or molecular coordinates and occupancies or quantities abstracted from these. The MC energy is calculated, and the system is perturbed (two site occupancies may be exchanged, an atom may be displaced, or two displacements may be exchanged, and so on) and the energy is recalculated. If the new configuration is of lower energy than the initial, the move is accepted. If not, the move may be accepted or rejected according to some probability that depends on the change in energy and the temperature, *T*.[40,44] After many thousands of such steps, the system can be brought into thermal equilibrium. The model interactions will cause correlations to propagate through the model, resulting in short-range order and, if the model is Fourier transformed appropriately,[45] producing diffuse scattering that can be compared with observations. This process may be embedded within an automated refinement procedure. This adjusts the parameters of the energy functions by quantitatively comparing the calculated diffuse scattering to the data and using some algorithm (for example, least-squares or genetic algorithms[46,47]) to obtain a fit to the diffuse scattering[48,49] (example diffuse scattering sections are shown in Figure 2). If the model energy is a reasonable facsimile of the real interactions in the material, the resulting model crystal is likely to be physically and chemically reasonable.

RMC uses the quality of the fit of the calculated pattern to the observed directly as an MC "energy". The great advantage of this is that the model is refined directly against the data, the disadvantage is that the relatively time-consuming calculation of diffuse scattering must be undertaken quite frequently, and care must be taken to ensure that the model is chemically reasonable.[50−52] RMC has found wide use in modeling pair distribution function data (PDF), where the need to calculate the PDF at every RMC step is far less computationally demanding than the need to calculate large reciprocal space cuts or volumes.

PDF is widely used to interpret diffuse scattering from powders. In such an experiment, the 3D distribution of diffuse scattering is projected onto a single axis as a function of scattering vector magnitude, that is, a powder diffraction pattern. These data are carefully corrected and then transformed to give the PDF.

This is an extremely valuable technique and highly complementary to SCDS, especially when single crystals are not available, a common situation. It is also extremely useful in undertaking parametric studies, because data sets can be acquired very rapidly as a function of some variable, such as temperature. This Account focuses on SCDS, but there are many examples of the use of PDF in similar studies.[53,54]

More recently, with the increasing power of computers, it has become possible to calculate local ordering using

ab initio methods. Comprehensive methods such as density functional theory (DFT) are at present generally unable to determine local structure on a large enough sample of atoms; when correlations can persist for perhaps ten unit cells, a model must be at least $10 \times 10 \times 10$ unit cells in size and preferably much larger. DFT can provide insight into the average structure[55] and the need for disorder, but small models are prone to problems due to periodic boundary conditions. Molecular dynamics (MD) and similar approaches, perhaps using parametrized versions of potentials calculated using DFT, offer the possibility of calculating the SRO and therefore the diffuse scattering (and other physical quantities) from first principles.[52,56]

3. Local Order in the Pb-Based Ferroelectrics

In the early 1980s, it was put forward that structure containing a population of small polarized regions of several unit cells in size could explain index of refraction measurements on PLZT ($Pb_{1-3x/2}La_x$)(Zr_yTi_{1-y})O_3), as well as an apparent phase transition at a temperature, denoted T_d (the Burns temperature), considerably higher than that of the ferroelectric to paraelectric phase transition.[57]

This idea of small domains, referred to as polar nanoregions (PNRs), has become the dominant one in describing the SRO in these lead-based materials.[17,20,27,58−62] These are then related to the strong ferro- and piezoelectric effects seen in these materials.[63] A subtly different conception invokes "ferroelectric nanodomains" (FNDs).[64−66] PNRs are seen as embedded in a paraelectric matrix, while for FNDs, the domains occupy essentially the full volume of the crystal, and their growth is halted when FNDs of different orientations interact,[65] meaning that the geometry of domain walls becomes very important, because they occupy a large fraction of the crystal volume. Chemically, the advantage of the FND picture over the PNR is that it is difficult to justify why some fraction of the crystal should be nonpolar and some fraction polar when the chemistry is the same; the only chemical inhomogeneity is the B-site randomness, which is extremely localized, even on the size-scale of a typical domain. In the FND picture, essentially all the crystal is behaving identically, in that all Pb^{2+} are part of a domain or a wall, and it is the independent nucleation of domains of different orientations, which possibly *does* relate to B-site inhomogeneity, since nucleation may be a very local phenomenon, that prevents the polar ordering from becoming long-ranged.

Many of the materials show evidence of a morphotropic phase boundary[67] (MPB) as a function of doping, often doping with $PbTiO_3$. For example, PZN-PT shows an MPB at $x \approx 0.09$,[68] PMN-PT at $x \approx 0.3$,[69] and $PbZr_{1-x}Ti_xO_3$ at $x \approx 0.47$.[70] At the MPB, the system is on the cusp between phases, and this results in increased ferro- and piezoelectric response. Because they are generally induced by doping, the MPB and the relaxor properties are frequently linked to chemical disorder.[71] However, an MPB has been discovered in pure $PbTiO_3$ as a function of pressure rather than doping. This suggests that the MPB may not really be related to the randomness linked to the doping but to the chemical pressure of differing ionic sizes. However, if we consider PZN-PT as PT doped with PZN, it is clear that substituting Nb and Zn onto the B-site results in a negative pressure on the A-site, since Nb^{5+} and Zn^{2+} are both larger than Ti^{4+}. Thus, doping PT with PZN acts to expand the unit cell, while applying pressure to PT will contract the structure. This agrees that an MPB may result from chemical pressure but shows that the pressure and chemically induced phase transitions are quite separate in the pressure manifold. It also does not preclude the chemical disorder being of significance in determining the properties of the system.

A number of ideas have been used to explain diffuse scattering in the Pb-based materials. In terms of interpretation, there are some commonalities between materials. Figure 5 shows two different reciprocal space cuts, from different compositions of $PbZr_{1-x}Ti_xO_3$, measured using electron diffraction. Both show streaks through reciprocal space. By comparing different zones it is possible to deduce that the streaks are in fact sections through planes of scattering.[25,26] One model for these planes is to assume that the Pb^{2+} ions assemble into 1D domains.

Using high temperature powder diffraction at a synchrotron, it has been shown that for $x = 0$ ($PbZrO_3$), the Pb^{2+} ions are on average split across the 12 $\langle 110 \rangle_c$ directions, where *c* indicates indexing based on the parent cubic structure.[24] This is noted on Figure 6 and illustrated by a cartoon in Figure 4. At other compositions, the disorder is across the 8 $\langle 111 \rangle_c$ directions, in accord with neutron diffraction.[72] The diffuse scattering can be modeled with this in mind[25,26] by disordering the Pb^{2+} across the appropriate sites then using an MC simulation to induce the suspected correlation structure, in this case, 1D domains of aligned displacements. The diffuse scattering can be calculated and compared with the data. Allowing that these data were collected using electron diffraction and are thus more qualitative than quantitative, it appears that the model does indeed reproduce many of the observed details (Figure 5c).

Why should the Pb^{2+} displace? For the $x = 0.3$ composition (Figure 5a), the preferred lattice parameter according to

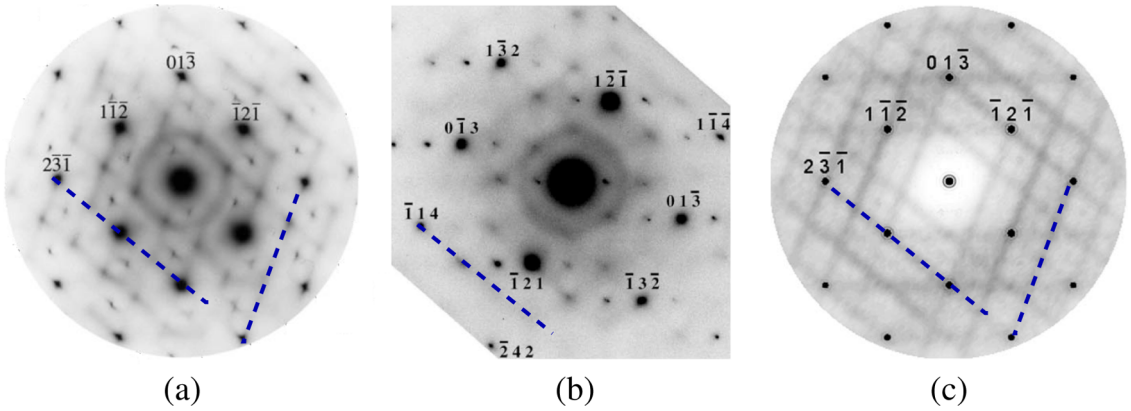

FIGURE 5. TEM images of electron diffuse scattering from PZT with streaks of scattering (really sections through planes) highlighted by dashed lines. (a) $PbZr_{1-x}Ti_xO_3$ with $x = 0.3$ (rhombohedral phase), viewed down the $[531]_c$ zone axis (c means relative to the cubic parent structure). (b) $x = 0.46$ (monoclinic) viewed down $[731]_c$. (c) Calculated pattern for the section in panel a, based on the MC model described in the text.[25,26]

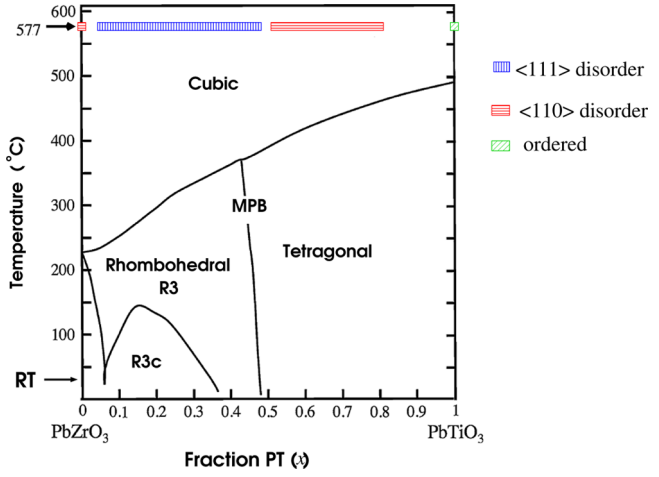

FIGURE 6. A schematic phase diagram for $PbTiO_3$, showing the main phases. The band across the top notes the x values for which different types of disordered arrangement of Pb^{2+} ions have been deduced at 850 K, well into the cubic phase.[24]

the B-site occupancy, a_B, based on bond-valence considerations,[73,74] is ~4.1 Å. This is derived from a weighted average of the Zr–O and Ti–O distances for 4+ ions in 6-fold coordination environments, such that each bond is expected to possess 4/6 valence units. The same calculation, using Pb^{2+} in a 12-fold environment gives $a_A \approx 3.92$ Å (observed lattice parameters for tetragonal $x = 0.3$ at room temperature are $a = 4.081$ Å and $c = 4.100$ Å,[75] showing how the B-site chemistry dominates). The Pb^{2+} is in an environment larger than desirable but the Pb^{2+}–O bond is "softer" than the B–O bonds,[74] meaning that the B–O preferred distance has a greater influence on the final lattice parameter, in agreement with observation.[23] The Pb^{2+} then moves off center to satisfy its bonding requirements. Hence, there is a relatively straightforward chemical reason as to why the Pb^{2+} is not at the center of its coordination volume. The same argument holds in PZN, PMN, and so on.

Figure 7 shows several cuts of diffuse scattering for PZN. Again, there are strong streaks of scattering, in this case rods rather than sections through planes, running in $\langle 110 \rangle_c$ directions. As rods, they can be generated by 2D domains, again of Pb^{2+} displacements,[76] each domain a single layer of atoms thick and oriented perpendicular to one of the $\langle 110 \rangle_c$ directions. PMN shows similar scattering.[77] Analysis often centers on the diffuse scattering around the Bragg positions (the so-called "butterfly" scattering) and tends to ignore the fact that the scattering is extended in reciprocal space. The rods are weaker in PMN but present. Similar scattering has been seen in $PbSc_{0.5}Nb_{0.5}O_3$ (PSN) and $PbSc_{0.5}Ta_{0.5}O_3$ (PST) and is interpreted with reference to PNRs.[78] Unlike PMN and PZN, in PSN and PST, the two B-site cations are in equal proportions, allowing strong B-site order. In these materials, *unlike* PZN and PMN, the $\langle 110 \rangle_c$ rods sharpen markedly on cooling and virtually disappear, presumably as any thermally induced disorder among Pb displacements weakens. In doped PSN, the diffuse rods are more strongly maintained on cooling.[79] Hence, in the systems where the disorder is chemically fixed and cannot vary with T, the diffuse rods are maintained. This suggests strongly that while the rods are indeed the result of correlated Pb displacements, the range of these correlations is limited by chemical disorder, in the case of PZN, PMN, and doped PST and PSN, whereas in undoped PSN and PST, the range of correlations depends on thermal agitation and so more strongly depends on temperature. Chemical disorder will result in small scale inhomogeneity in electric field due to the different charges on Zn^{2+} and Nb^{5+} or Mg^{2+} and Nb^{5+}, for example, and local strains due to differing atomic sizes.

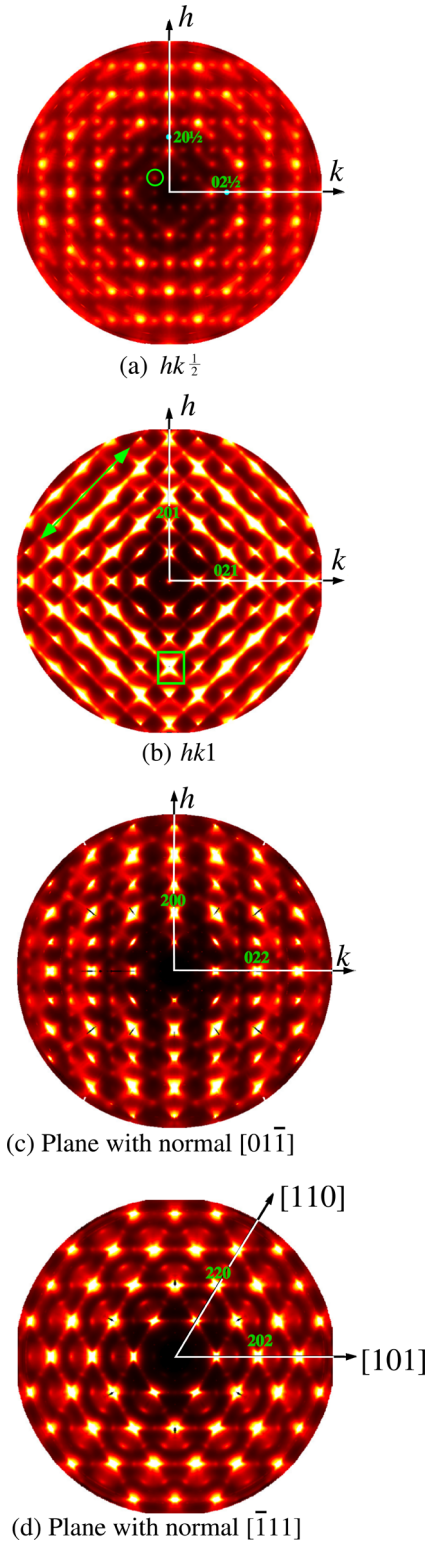

FIGURE 7. Synchrotron X-ray diffuse scattering images from PZN, $PbZn_{1/3}Nb_{2/3}O_3$, at 100 K, showing the strong streaks of diffuse scattering (an example is marked with an arrow in panel b), plus spots due to short-range Nb^{5+}/Zn^{2+} ordering (an example is circled in panel a; other spots are due to the intersection of diffuse rods). Axes are labeled and some diffraction positions noted for scale.

Thus, it is tempting to describe the local order in the Pb-based relaxors as the result of the need for the Pb to displace off-center, coupled with chemical disorder that prevents the ferroelectric order from extending beyond the nanoscale. Why the ferroelectric correlations should form into plate-like domains has been tackled using *ab initio* calculations, which shed light not only on the drivers for the ordering but also on the interpretability of diffuse scattering data.

MC modeling had initially suggested that the Pb^{2+} displacements should be in $\langle 110\rangle_c$ directions to account for the lack of streak intensity at the origin.[62] It has since been shown that the diffuse scattering can be modeled without assuming $\langle 110\rangle_c$ atomic shifts, as long as the "relative inter-domain displacement vector" is "perpendicular to $\langle 110\rangle_c$".[56] Molecular dynamics modeling of PMN suggests that at ~10 K the Pb^{2+} prefer to displace onto $\langle 111\rangle_c$ positions, a distribution that becomes less well-defined as the system is warmed up.[80] A recent PDF study of PZN suggests that $\langle 110\rangle_c$ displacements are most likely,[81] while the Bragg average structures of both PZT and PZN-PT show changes in the disorder ($\langle 110\rangle_c$ or $\langle 111\rangle_c$) as a function of doping.[24,82] This suggests that while it may be *possible* to model the diffuse scattering with a wide range of displacement distributions, the real distribution will be sensitive to the crystal chemistry such that one choice of displacement type (combined with conventional ADPs) will provide the best approximation.

Diffuse scattering "depends on spatially and temporally averaged pair correlations only",[65] which means that the presence of $\langle 110\rangle_c$ rods need not imply static domains of displaced atoms. Key features of the diffuse scattering can be modeled using a thermal-like picture,[32,83,84] which works well for the "butterfly"-like motifs around some Bragg positions (an example butterfly is shown in the boxed area in Figure 7b). The model makes use of parameters that are analogous to elastic constants without being such. The resulting fit uses only a handful of parameters and is impressive in some aspects. It is a powerful indication of how the intuitive approach can at times be misleading.

Atomistic molecular dynamics (MD) simulations also do not imply static plate-like layers of atoms but show that strongly anisotropic cooperative displacement behavior can reproduce the observed diffuse scattering. This behavior is revealed by examining conditional probabilities (related to pair correlations). The local strain due to different sizes of the B-site cations is integral to this model, more so than random electric fields, which is interesting information in the search for new compounds.[80]

The conventional "domain" view can be thought of as a snapshot of these more dynamic models, which is why it

also can be used to fit the data and why it is still valid in obtaining chemical insight. These insights include the need for the inherent polarity of the Pb^{2+} ion, the size of the Pb^{2+} environment relative to its preferred environment (one in which it could remain centered), the degree of order of the B-site cations, and the relative sizes of the B-site cations.

As temperatures increase, the role of thermal vibrations (phonons) becomes significant. Long-range, dispersive lattice modes will relate to the average structure and must be allowed for when trying to determine what effects are due to the local chemistry. Temperature-dependent studies aid in this,[85] as do studies of lattice dynamics and energy-analyzed diffuse scattering using neutrons.[86]

4. Conclusions

The Pb^{2+}-based ferroelectrics, particularly the relaxors, show a wide range of complex behavior. This relates to the wide variety of local structures, including chemical short-range order, correlated atomic displacements, and the atomic size effect.[85] Some of these local orderings can be captured by a phonon-like picture, others through a real-space, empirical, atomistic simulation. These approaches deliver *descriptions* of the local ordering, and from these some important attributes of the chemistry can be inferred. However, it is clear that there are aspects both of order−disorder and of phonon-related behavior in these materials. Hence, detailed modeling of the local order and the "domain" structure requires the precision of a quantum mechanical technique like density functional theory yet also requires study of a sufficiently large system that a statistically valid population of local configurations can be generated, a model much too large for a DFT calculation. Molecular dynamics based on parametrization of potentials derived from detailed calculations offers a powerful way to work around these issues and delivers detailed insights.

It is also apparent that the diffuse scattering alone cannot constrain the model sufficiently, for example, in determining the absolute displacement direction of the Pb^{2+} ions. Other data, including high-quality long-range average structure determinations and the principles of crystal chemistry (whether bond valence sums and tolerance factors or quantum chemical calculations), must be employed.

A great benefit of the development of more chemically and physically reasonable models is that many quantities can be sensibly calculated from them. This leads to a model crystal being "refined" against multiple data sets, diffuse scattering, Bragg scattering, XAFS, thermodynamic measurements, phonon dispersion, Raman, Mössbauer, and so on, resulting in a potentially unprecedented level of structural detail. When structure and function are being calculated from the same model, the ability to understand materials and then design new ones is greatly enhanced. And, clearly, in many materials, it is not adequate to base such modeling on the long-range average structure. Detailed modeling of the local order is essential if we are to understand the mechanisms at work in these useful and interesting materials.

The most common ion used as a replacement for Pb^{2+} is Bi^{3+}, a similarly heavy ion with a lone pair. Sn^{2+} also possesses the lone pair, though its chemistry is difficult. When we better understand how the average and local chemistry combine to drive the Pb^{2+} behavior, from relatively simple effects like the size of the ion site relative to its "preferred" bond length through to random field effects due to B-site substitution and on to subtle quantum mechanical effects,[87] we will be able to design a perovskite, including "designing the disorder", such that Bi^{3+} (or Sn^{2+}) will be induced to behave as we require. This will herald a powerful new tool not just in the study of ferroic materials but in materials science more broadly.

The author thanks the Australian Research Council for support through its Discovery Projects program. He also thanks Dr. A. P. Heerdegen, Prof. T. R. Welberry, Prof. R. L. Withers, Dr. Marek Paściak, Dr. Jessica Hudspeth, and Ross Whitfield of the Research School of Chemistry at the Australian National University for their advice and contributions to collection of data. They are responsible for none of the errors and omissions herein, however. Use of the Advanced Photon Source, an Office of Science User Facility operated for the U.S. Department of Energy (DOE) Office of Science by Argonne National Laboratory, was supported by the U.S. DOE under Contract No. DE-AC02-06CH11357.

FOOTNOTES

*E-mail: goossens@rsc.anu.edu.au. Phone: +61 2 6125 3536. Fax: +61 2 6125 0750.
The author declares no competing financial interest.

REFERENCES

1 Park, S.-E. E.; Hackenberger, W. High performance single crystal piezoelectrics: Applications and issues. *Curr. Opin. Solid State Mater. Sci.* **2002**, *6*, 11–18.
2 Gururaja, T. R.; K, R.; Panda; Chen, J.; Beck, H. Single crystal transducers for medical imaging applications. *Proc. - IEEE Ultrason. Symp.* **1999**, 969–972.
3 Pruvost, S.; Hajjaji, A.; Lebrun, L.; Guyomar, D.; Boughaleb, Y. Domain switching and energy harvesting capabilities in ferroelectric materials. *J. Phys. Chem. C* **2010**, *114*, 20629–20635.
4 Lebrun, L.; Sebald, G.; Guiffard, B.; Richard, C.; Guyomar, D.; Pleska, E. Investigations on ferroelectric PMN-PT and PZN-PT single crystals ability for power or resonant actuators. *Ultrasonics* **2004**, *42*, 501–505.
5 Cross, L. E. Ferroelectric materials for electromechanical transducer applications. *Mater. Chem. Phys.* **1996**, *43*, 108–115.
6 Young, C. A.; Goodwin, A. L. Applications of pair distribution function methods to contemporary problems in materials chemistry. *J. Mater. Chem.* **2011**, *21*, 6464–6476.

7 Playford, H. Y.; Hannon, A. C.; Barney, E. R.; Walton, R. I. Structures of uncharacterised polymorphs of gallium oxide from total neutron diffraction. *Chem.—Eur. J.* **2013**, *19*, 2803–2813.

8 Barabash, R. I., Ice, G. E., Turchi, P. E. A., Eds. *Diffuse Scattering and the Fundamental Properties of Materials*, 1st ed.; Momentum Press: New York, 2009.

9 Butler, B. D.; Welberry, T. R. Interpretation of displacement-caused diffuse scattering using the Taylor expansion. *Acta Crystallogr.* **1993**, *49*, 736–743.

10 Warren, B. E.; Averbach, B. L.; Roberts, B. W. Atomic size effect in the X-ray scattering by alloys. *J. Appl. Phys.* **1951**, *22*, 1493–1496.

11 Hicks, T. J. Experiments with neutron polarization analysis. *Adv. Phys.* **1996**, *45*, 243–298.

12 Goossens, D. J.; James, D.; Dong, J.; Whitfield, R. E.; Norén, L.; Withers, R. L. Local order in layered $NiPS_3$ and $Ni_{0.7}Mg_{0.3}PS_3$. *J. Phys.: Condens. Matter* **2011**, *23*, No. 065401.

13 Harburn, G.; Taylor, C. A.; Welberry, T. R. *Atlas of Optical Transforms*; Bell: London, 1975.

14 Bordat, P.; Brown, R. A molecular model of p-terphenyl and its disorder-order transition. *Chem. Phys.* **1999**, *246*, 323–334.

15 Baudour, P. J.-L.; Cailleau, H.; Yelon, W. B. Structural phase transition in polyphenyls. IV. Double-well potential in the disordered phase of p-terphenyl from neutron (200 K) and X-ray (room-temperature) diffraction data. *Acta Crystallogr.* **1977**, *B33*, 1773–1780.

16 Goossens, D. J.; Beasley, A. G.; Welberry, T. R.; Gutmann, M. J.; Piltz, R. O. Neutron diffuse scattering in deuterated para-terphenyl, $C_{18}D_{14}$. *J. Phys.: Condens. Matter* **2009**, *21*, No. 124204.

17 Welberry, T. R.; Goossens, D. J. Different models for the polar nanodomain structure of PZN and other relaxor ferroelectrics. *J. Appl. Crystallogr.* **2008**, *41*, 606–614.

18 Amin, A.; Newnham, R.; Cross, L.; Cox, D. Phenomenological and structural study of a low-temperature phase transition in the $PbZrO_3-xPbTiO_3$ system. *J. Solid State Chem.* **1981**, *37*, 248–255.

19 Rouquette, J.; Haines, J.; Fraysse, G.; Al-Zein, A.; Bornand, V.; Pintard, M.; Papet, P.; Hull, S.; Gorelli, F. A. High-pressure structural and vibrational study of $PbZr_{0.40}Ti_{0.60}O_3$. *Inorg. Chem.* **2008**, *47*, 9898–9904.

20 Frantti, J. Notes of the recent structural studies on lead zirconate titanate. *J. Phys. Chem. B* **2008**, *112*, 6521–6535.

21 Longo, E.; de Figueiredo, A. T.; Silva, M. S.; Longo, V. M.; Mastelaro, V. R.; Vieira, N. D.; Cilense, M.; Franco, R. W. A.; Varela, J. A. Influence of structural disorder on the photoluminescence emission of PZT powders. *J. Phys. Chem. A* **2008**, *112*, 8953–8957.

22 Frantti, J.; Ivanov, S.; Eriksson, S.; Lappalainen, J.; Lantto, V.; Kakihana, M.; Rundlöf, H. Neutron diffraction and bond-valence calculation studies of $Pb(Zr_xTi_{1-x})O_3$ ceramics. *Ferroelectrics* **2002**, *272*, 51–56.

23 Yokota, H.; Zhang, N.; Taylor, A. E.; Thomas, P. A.; Glazer, A. M. Crystal structure of the rhombohedral phase of $PbZr_{1-x}Ti_xO_3$ ceramics at room temperature. *Phys. Rev. B* **2009**, *80*, No. 104109.

24 Kuroiwa, Y.; Terado, Y.; Kim, S. J.; Sawada, A.; Yamamura, Y.; Aoyagi, S.; Nishibori, E.; Sakata, M.; Takata, M. High-energy SR powder diffraction evidence of multisite disorder of Pb atom in cubic phase of $PbZr_{1-x}Ti_xO_3$. *Jpn. J. Appl. Phys.* **2005**, *44*, 7151–7155.

25 Welberry, T.; Goossens, D.; Withers, R.; Baba-Kishi, K. Monte Carlo simulation study of diffuse scattering in PZT, $Pb(Zr,Ti)O_3$. *Metall. Mater. Trans. A* **2010**, *41*, 1110–1118.

26 Baba-Kishi, K. Z.; Welberry, T. R.; Withers, R. L. An electron diffraction and Monte Carlo simulation study of diffuse scattering in $Pb(Zr,Ti)O_3$. *J. Appl. Crystallogr.* **2008**, *41*, 930–938.

27 Glazer, A. M.; Thomas, P. A.; Baba-Kishi, K. Z.; Pang, G. K. H.; Tai, C. W. Influence of short-range and long-range order on the evolution of the morphotropic phase boundary in $Pb(Zr_{1-x}Ti_x)O_3$. *Phys. Rev. B* **2004**, *70*, No. 184123.

28 Burkovsky, R. G.; Bronwald, Y. A.; Filimonov, A. V.; Rudskoy, A. I.; Chernyshov, D.; Bosak, A.; Hlinka, J.; Long, X.; Ye, Z.-G.; Vakhrushev, S. B. Structural heterogeneity and diffuse scattering in morphotropic lead zirconate-titanate single crystals. *Phys. Rev. Lett.* **2012**, *109*, No. 097603.

29 Krivoglaz, M. A. *Theory of X-ray and Thermal-Neutron Scattering by Real Crystals*; Plenum Press: New York, 1969.

30 Cowley, J. M. Short-range order and long-range order parameters. *Phys. Rev.* **1965**, *138*, A1384–A1389.

31 Dove, M.; Hammonds, K.; Heine, V.; Withers, R.; Xiao, Y.; Kirkpatrick, R. Rigid unit modes in the high-temperature phase of SiO_2 tridymite: calculations and electron diffraction. *Phys. Chem. Miner.* **1996**, *23*, 56–62.

32 Bosak, A.; Chernyshov, D.; Vakhrushev, S.; Krisch, M. Diffuse scattering in relaxor ferroelectrics: True three-dimensional mapping, experimental artefacts and modelling. *Acta Crystallogr.* **2012**, *A68*, 117–123.

33 Paściak, M.; Wołcyrz, M.; Pietraszko, A. Interpretation of the diffuse scattering in Pb-based relaxor ferroelectrics in terms of three-dimensional nanodomains of the <110>-directed relative interdomain atomic shifts. *Phys. Rev. B* **2007**, *76*, No. 014117.

34 Neder, R. B.; Proffen, T. *Diffuse Scattering and Defect Structure Simulations: A cook book using the program DISCUS*; Oxford University Press: Oxford, U.K., 2008.

35 Neder, R. B.; Wildgruber, U. DISCUS, ein Interaktives Programm zur Simulation von Defektstrukturen und Diffuser Streuung. *Z. Kristallogr.* **1989**, *186*, 209 (in German).

36 Goossens, D. J.; Heerdegen, A. P.; Chan, E. J.; Welberry, T. R. Monte Carlo modelling of diffuse scattering from single crystals: The Program ZMC. *Metall. Mater. Trans. A* **2010**, *42A*, 23–31.

37 Weber, T.; Simonov, A. The three-dimensional pair distribution function analysis of disordered single crystals: basic concepts. *Z. Kristallogr.* **2012**, *227*, 238–247.

38 Michels-Clark, T.; Chodkiewicz, M.; Hoffmann, C.; Hauser, J.; Linden, A.; Lynch, V.; Weber, T.; Bürgi, H.-B. Modeling diffuse scattering using evolutionary algorithms and super computing. *Acta Crystallogr.* **2011**, *A67*, No. C77.

39 Withers, R. L.; Liu, Y.; Welberry, T. Structured diffuse scattering and the fundamental 1-d dipolar unit in PLZT $(Pb_{1-y}La_y)_{1-\alpha}(Zr_{1-x}Ti_x)_{1-\beta}O_3$ (7.5/65/35 and 7.0/60/40) transparent ferroelectric ceramics. *J. Solid State Chem.* **2009**, *182*, 348–355.

40 Welberry, T. *Diffuse X-ray Scattering And Models Of Disorder*; International Union of Crystallography Monographs on Crystallography 16; Oxford University Press: Oxford, U.K., 2004.

41 Welberry, T. R.; Butler, B. D. Diffuse X-ray scattering from disordered crystals. *Chem. Rev.* **1995**, *95*, 2369–2403.

42 Metropolis, N.; Rosenbluth, A. W.; Rosenbluth, M. N.; Teller, A. H.; Teller, E. Equation of state calculations by fast computing machines. *J. Chem. Phys.* **1953**, *21*, 1087–1092.

43 Nield, V. M.; Keen, D. A.; McGreevy, R. L. The interpretation of single-crystal diffuse scattering using reverse Monte Carlo modelling. *Acta Crystallogr.* **1995**, *A51*, 763–771.

44 Schweika, W. *Disordered Alloys: Diffuse Scattering and Monte Carlo Simulations*; Springer: Berlin, 1998.

45 Butler, B. D.; Welberry, T. R. Calculation of diffuse scattering from simulated crystals: A comparison with optical transforms. *J. Appl. Crystallogr.* **1992**, *25*, 391–399.

46 Weber, T.; Bürgi, H.-B. Determination and refinement of disordered crystal structures using evolutionary algorithms in combination with Monte Carlo methods. *Acta Crystallogr.* **2002**, *A58*, 526–540.

47 Bürgi, H.-B.; Weber, T. The structural complexity of a polar, molecular material brought to light by synchrotron radiation. *Mol. Cryst. Liq. Cryst.* **2003**, *390*, 1–4.

48 Welberry, T. R.; Proffen, T.; Bown, M. Analysis of single-crystal diffuse X-ray scattering via automatic refinement of a Monte Carlo model. *Acta Crystallogr.* **1998**, *A54*, 661–674.

49 Goossens, D. J.; Welberry, T. R.; Heerdegen, A. P.; Gutmann, M. J. Simultaneous fitting of X-ray and neutron diffuse scattering data. *Acta Crystallogr.* **2007**, *A63*, 30–35.

50 Beverley, M. N.; Nield, V. M. Extensive tests on the application of reverse Monte Carlo modelling to single-crystal neutron diffuse scattering from ice Ih. *J. Phys.: Condens. Matter* **1997**, *9*, No. 5145.

51 McGreevy, R. L. Reverse Monte Carlo modelling. *J. Phys.: Condens. Matter* **2001**, *13*, No. R877.

52 Paściak, M.; Heerdegen, A.; Goossens, D.; Whitfield, R.; Pietraszko, A.; Welberry, T. Assessing local structure in $PbZn_{1/3}Nb_{2/3}O_3$ using diffuse scattering and reverse Monte Carlo refinement. *Metall. Mater. Trans. A* **2013**, *44*, 87–93.

53 Egami, T. In *Ferro- and Antiferroelectricity*; Dalal, N., Bussmann-Holder, A., Eds.; Structure and Bonding; Springer: Berlin Heidelberg, 2007; Vol. 124; pp 69—88.

54 Kwei, G. H.; Billinge, S. J. L.; Cheong, S.-W.; Saxton, J. G. Pair-distribution functions of ferroelectric perovskites: Direct observation of structural ground states. *Ferroelectrics* **1995**, *164*, 57–73.

55 Rodriguez, J. A.; Etxeberria, A.; Gonzalez, L.; Maiti, A. Structural and electronic properties of $PbTiO_3$, $PbZrO_3$, and $PbZr_{0.5}Ti_{0.5}O_3$: First-principles density-functional studies. *J. Chem. Phys.* **2002**, *117*, 2699–2709.

56 Paściak, M.; Welberry, T. R. Diffuse scattering and local structure modeling in ferroelectrics. *Z. Kristallogr.* **2011**, *226*, 113–125.

57 Burns, G.; Dacol, F. H. Crystalline ferroelectrics with glassy polarization behavior. *Phys. Rev. B* **1983**, *28*, 2527–2530.

58 Xu, G.; Zhong, Z.; Bing, Y.; Ye, Z.-G.; Shirane, G. Electric-field-induced redistribution of polar nano-regions in a relaxor ferroelectric. *Nat. Mater.* **2006**, *5*, 134–140.

59 Xu, G.; Wen, J.; Stock, C.; Gehring, P. M. Phase instability induced by polar nanoregions in a relaxor ferroelectric system. *Nat. Mater.* **2008**, *7*, 562–566.

60 Cohen, J. B. Relaxors go critical. *Nature* **2006**, *441*, 941–942.

61 Deluca, M.; Pezzotti, G. First-order transverse phonon deformation potentials of tetragonal perovskites. *J. Phys. Chem. A* **2008**, *112*, 11165–11171.

62 Welberry, T. R.; Gutmann, M. J.; Woo, H.; Goossens, D. J.; Xu, G.; Stock, C.; Chen, W.; Ye, Z.-G. Single-crystal neutron diffuse scattering and Monte Carlo study of the relaxor ferroelectric $PbZn_{1/3}Nb_{2/3}O_3$ (PZN). *J. Appl. Crystallogr.* **2005**, *38*, 639–647.

63 Bokov, A.; Ye, Z.-G. Recent progress in relaxor ferroelectrics with perovskite structure. *J. Mater. Sci.* **2006**, *41*, 31–52.

64 Maksymovych, P.; Morozovska, A. N.; Yu, P.; Eliseev, E. A.; Chu, Y.-H.; Ramesh, R.; Baddorf, A. P.; Kalinin, S. V. Tunable metallic conductance in ferroelectric nanodomains. *Nano Lett.* **2012**, *12*, 209–213.

65 Hlinka, J. Do we need the ether of polar nanoregions? *J. Adv. Dielectr.* **2012**, *2*, No. 1241006.

66 Paściak, M.; Boulfelfel, S. E.; Leoni, S. Polarized cluster dynamics at the paraelectric to ferroelectric phase transition in $BaTiO_3$. *J. Phys. Chem. B* **2010**, *114*, 16465–16470.

67 Ahart, M.; Somayazulu, M.; Cohen, R. E.; Ganesh, P.; Dera, P.; Mao, H.-k.; Hemley, R. J.; Ren, Y.; Liermann, P.; Wu, Z. Origin of morphotropic phase boundaries in ferroelectrics. *Nature* **2008**, *451*, 545–548.

68 El Marssi, M.; Dammak, H. Orthorhombic and monoclinic ferroelectric phases investigated by Raman spectroscopy in PZN-4.5%PT and PZN-9%PT crystals. *Solid State Commun.* **2007**, *142*, 487–491.

69 Choi, S.; Shrout, T.; Jang, S.; Bhalla, A. Morphotropic phase boundary in $Pb(Mg_{1/3}Nb_{2/3})O_3$-$PbTiO_3$ system. *Mater. Lett.* **1989**, *8*, 253–255.

70 Kuwata, J.; Uchino, K.; Nomura, S. Phase transitions in the $Pb(Zn_{1/3}Nb_{2/3})O_3$-$PbTiO_3$ system. *Ferroelectrics* **1981**, *37*, 579–582.

71 Davies, P.; Akbas, M. Chemical order in PMN-related relaxors: structure, stability, modification, and impact on properties. *J. Phys. Chem. Solids* **2000**, *61*, 159–166.

72 Corker, D. L.; Glazer, A. M.; Whatmore, R. W.; Stallard, A.; Fauth, F. A neutron diffraction investigation into the rhombohedral phases of the perovskite series $PbZr_{1-x}Ti_xO_3$. *J. Phys.: Condens. Matter* **1998**, *10*, No. 6251.

73 Brese, N. E.; O'Keeffe, M. Bond-valence parameters for solids. *Acta Crystallogr.* **1991**, *B47*, 192–197.

74 Brown, I. D. Recent developments in the methods and applications of the bond valence model. *Chem. Rev.* **2009**, *109*, 6858–6919.

75 Shirane, G.; Suzuki, K.; Takeda, A. Phase transitions in solid solutions of $PbZrO_3$ and $PbTiO_3$ (II) X-ray study. *J. Phys. Soc. Jpn.* **1952**, *7*, 12–18.

76 Welberry, T. R. Diffuse scattering and Monte Carlo studies of relaxor ferroelectrics. *Metall. Mater. Trans. A* **2008**, *39*, 3170–3178.

77 You, H.; Zhang, Q. M. Diffuse X-ray scattering study of lead magnesium niobate single crystals. *Phys. Rev. Lett.* **1997**, *79*, 3950–3953.

78 Mihailova, B.; Angel, R. J.; Welsch, A.-M.; Zhao, J.; Engel, J.; Paulmann, C.; Gospodinov, M.; Ahsbahs, H.; Stosch, R.; Güttler, B.; Bismayer, U. Pressure-induced phase transition in $PbSc_{0.5}Ta_{0.5}O_3$ as a model Pb-based perovksite-type relaxor ferroelectric. *Phys. Rev. Lett.* **2008**, *101*, No. 017602.

79 Maier, B.; Mihailova, B.; Paulmann, C.; Ihringer, J.; Gospodinov, M.; Stosch, R.; Güttler, B.; Bismayer, U. Effect of local elastic strain on the structure of Pb-based relaxors: A comparative study of pure and Ba- and Bi-doped $PbSc_{0.5}Nb_{0.5}O_3$. *Phys. Rev. B* **2009**, *79*, No. 224108.

80 Paściak, M.; Welberry, T. R.; Kulda, J.; Kempa, M.; Hlinka, J. Polar nanoregions and diffuse scattering in the relaxor ferroelectric $PbMg_{1/3}Nb_{2/3}O_3$. *Phys. Rev. B* **2012**, *85*, No. 224109.

81 Whitfield, R. E. Diffuse scattering study of short-range order in lead zinc niobate. Ph.D. thesis, Australian National University, 2013.

82 Terado, Y.; Kim, S. J.; Moriyoshi, C.; Kuroiwa, Y.; Iwata, M.; Takata, M. Disorder of Pb atom in cubic structure of $Pb(Zn_{1/3}Nb_{2/3})O_3-PbTiO_3$ system. *Jpn. J. Appl. Phys.* **2006**, *45*, 7552–7555.

83 Bosak, A.; Chernyshov, D. On model-free reconstruction of lattice dynamics from thermal diffuse scattering. *Acta Crystallogr.* **2008**, *A64*, 598–600.

84 Chernyshov, D.; Bosak, A.; Vakhrushev, S.; Krisch, M. A new model of correlated disorder in relaxor ferroelectrics. *Acta Crystallogr.* **2008**, *A67*, C78.

85 Whitfield, R. E.; Goossens, D. J.; Studer, A. J. Temperature dependence of diffuse scattering in PZN. *Metall. Mater. Trans. A* **2012**, *43A*, 1429–1433.

86 Gehring, P. M.; Hiraka, H.; Stock, C.; Lee, S.-H.; Chen, W.; Ye, Z.-G.; Vakhrushev, S. B.; Chowdhuri, Z. Reassessment of the Burns temperature and its relationship to the diffuse scattering, lattice dynamics, and thermal expansion in relaxor $Pb(Mg_{1/3}Nb_{2/3})O_3$. *Phys. Rev. B* **2009**, *79*, No. 224109.

87 Payne, D. J.; Egdell, R. G.; Walsh, A.; Watson, G. W.; Guo, J.; Glans, P.-A.; Learmonth, T.; Smith, K. E. Electronic origins of structural distortions in post-transition metal oxides: Experimental and theoretical evidence for a revision of the lone pair model. *Phys. Rev. Lett.* **2006**, *96*, No. 157403.